PHYSICAL NATURE OF STAGES IN PLASTIC DEFORMATION

N. A. Koneva and É. V. Kozlov   UDC 681.142:535

INTRODUCTION

The nature of the stages in plastic deformation is one of the main problems in the physics of plasticity and strength. It has been studied intensively for the past few decades. A number of reviews and monographs have been dedicated to this problem [1-6]. The last review appeared more than ten years ago. Moreover, major advances have been made recently in understanding the nature of the occurrence of plastic deformation in stages. Our aim is to generalize the advances of these years. This paper reports experimental results obtained mainly by us and our coworkers as well as a concept developed by comparing these data with the results of other workers.

The analysis is based on the idea of structural levels of deformation. The first clear idea of structural levels of a deformable solid was first introduced by Panin [7, 8]. On the basis of the results of different workers, in Table 1 we give our own version of the hierarchy of structural levels. We must emphasize that the structural levels do not function in isolation but, on the contrary, interact and the overall picture of deformation and hardening is a result of this interaction as well.

As the steps of the hierarchy of structural levels is ascended there is a transition from individual defects, especially dislocations, to groups of them and more complex formations; in this way collective effects, a higher manifestation of which is a dislocation (or even vacancy–dislocation–disclination) ensemble, appear and play an increasing role in the defect structure.

The inclusion of the dislocation ensemble among the structural levels requires particular elucidation. This concept incorporates micron portions of the material with considerable dislocation density, at least such that the interaction between individual dislocations and groups of them would be commensurate with the action of external stress on the dislocation and the dimension of the portion would be at least larger than the screening radius of the elastic field of the dislocations of groups of them. Under such conditions dislocations, tending to decrease the energy of their own total elastic field, can change their spatial position and form different substructures. As will be seen from the discussion below, many factors of plastic deformation and strain hardening will be determined by the types of substructure, i.e., by the structure and properties of the dislocation ensemble.

1. STAGES IN STRESS–STRAIN CURVES – A GENERAL
PROPERTY OF SINGLE CRYSTALS AND POLYCRYSTALS

The stress–strain (σ vs. ε) dependence for one material under a variety of conditions has been studied in greatest detail on the alloy Ni_3Fe. The functions $\sigma = f(\varepsilon)$ for this alloy were studied on single crystals with different orientations and on polycrystals over a wide range of grain size in ordered and disordered states at different temperatures [9-21]. Parallel tensile and compression tests established that the functions $\sigma = f(\varepsilon)$ differ insignificantly and the existence of stages manifested in them in the same way [12].

Analysis of the entire body of data obtained on this alloy showed that in the most general case $\sigma = f(\varepsilon)$ is a four-stage dependence (Fig. 1). Several stages are distinguished. A transitional stage (π), which comes after the yield stress and demonstrates either an increase or a decrease in the strain hardening coefficient $\Theta = d\sigma/d\varepsilon$. This is followed by stage II with a high constant, or almost constant, hardening coefficient. In the next stage, stage III, the hardening coefficient decreases and $\sigma = f(\varepsilon)$ is parabolic, or nearly so. This stage

TABLE 1. Structural Levels and Their Scale and Classification

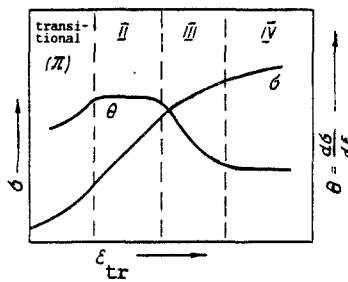| Designation	Scale
Microlevel	
1 Vacancy, atom	2—3 Å
2 Kink, threshold	5—50 Å
3 Dislocation, step on grain boundary, Crowdion	100 A
4 Dislocation group, tangle, slip bands, shear zone, dislocation wall, individual disclination-type formations. Grain boundary. Domain walls, Vacancy, atomic, and mixed clusters, segregations, and second-phase particles	100—1000 Å
Mesolevel	
5 Cell, disclination loop and dipole, band in band substructure, kink microband, microtwins, disclination groups. Martensite lamellae and rods. Mosaic block, fragment, subgrain	0,1—1,0 μm
6 Dislocation ensemble, Segment of grain or single crystal. Packet of martensite rods. Shear zones, slip system	1 μm — 20 μm
Grain level	
7 Grain. Dendrite. Shear zone, slip system	10—200 μm
Macrolevel	
8 Group of grain. Composite filament	0,2—0.5 μm
9 Portion of sample	1 μm
10 Sample as a whole	1 mm—1 cm

Fig. 1. Schematic representation of a typical four-stage stress—strain curve. The dashed lines indicate the stages of deformation.

sometimes can be divided into substages III and III', which differ as to their parabolicity coefficients. Finally, after stage III comes stage IV with a low, constant hardening coefficient.

This general picture can have a number of anomalies in the particular case. First, the transition from stage to stage can be abrupt or smeared and the behavior of the hardening coefficient in neighboring stages can differ either substantially or only slightly. Second, the transitional stage may be preceded by a stage of easy slip, stage I. It is observed only in single crystals with certain orientations. Third, more stages may be observed after stage IV. Thus far they have been studied only a little. Fourth, there exist unique anomalous cases when some of the main stages, e.g., stage II, are missing from the curves. We emphasize that the variation of the strain hardening coefficient with the deformation is quasioscillating in the general case: the types of stage are observed to alternate clearly — a stage with decreasing (or increasing) Θ, another stage with constant Θ, and so forth.

Let us consider the hardening law in greater detail. The function $\sigma = f(\varepsilon)$ of polycrystals with different grain size is graphed in Fig. 2. Clearly, the existence of stages in the stress—strain curves is a general property of polycrystals in range of grain sizes from 20 to 2000 μm, i.e., in the range corresponding to a grain-size variation of two orders of magnitude. The ordered state of the alloy is characterized by a more pronounced difference in the stages and an increase in Θ in the transitional stage; in the disordered alloy Θ decreases in that stage. The effect of the grain size is much weaker in the ordered state.
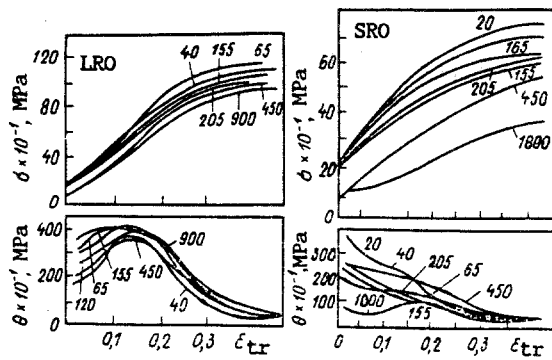
Fig. 2. Stress—strain curves σ vs ε_{tr} and Θ vs ε curves. The numbers next to the curves denote the grain size in μm (LRO is the long-range order; SRO is the short-range order, the disordered state).
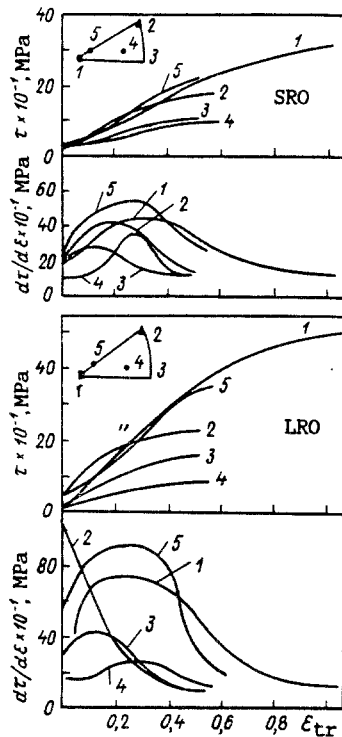

Fig. 3. Stress—strain curves and dτ/dε vs ε curves of single crystals of Ni_3Fe alloy with different orientations: 1) [001]; 2) [$\bar{1}$11]; 3) [011]; 4) [1.8.12]; 5) [119].

At a grain size of more than 1500 μm the function σ = f(ε) begins to take on the features of monocrystallinity.

The stress—strain curves of single crystals exhibit a wider variety of shapes. The main factor determining this diversity is the number of starting slip systems with equal loads. As for polycrystals, in the case of single crystals we confine the discussion to the dependences at room temperature and two limiting states of order. The corresponding compression stress—strain curves are shown in Fig. 3. The indicated testing method produces high degrees of deformation, corresponding to further stages.

This picture of a multistage process is characteristic of both single crystals and polycrystals. The transitional stage and stages II, III, and IV occurs in most orientations. Stage I in pure form is observed for orientations inside a stereographic triangle and with
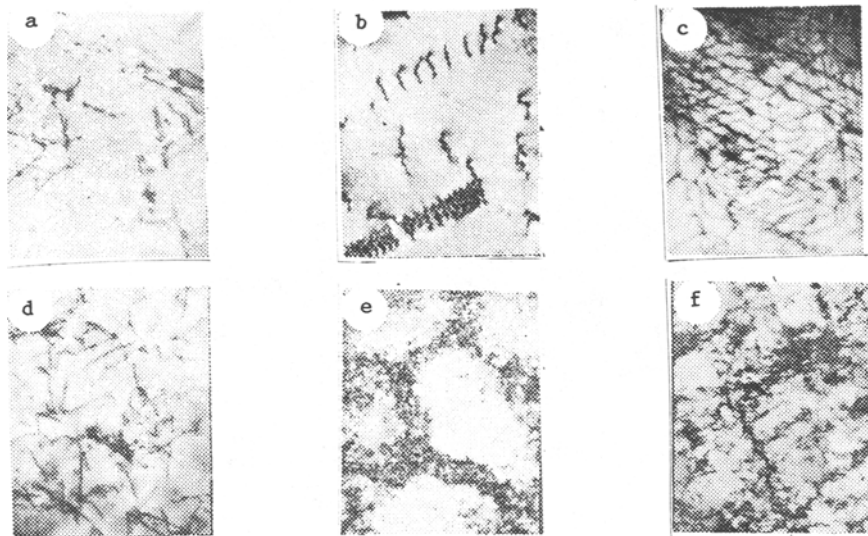
167

Fig. 4. Examples of types of non-misoriented dislocation substruc-
tures observed in fcc alloys.

a higher hardening coefficient on $[001]-[\bar{1}11]$ lines. Short segments of these stages are
also visible at some other orientations. Studies involving tests at other temperatures in
the range 77-900 K showed that the picture of a process in stages manifests itself clearly
at any temperature. It is most distinct for the [001], [119], and [1.8.12] orientations.
In the $[\bar{1}11]$ orientation for a disordered alloy and the [011] orientation for both states
of order the transition from stage to stage is less abrupt and, finally, in an ordered state
with the $[\bar{1}11]$ orientation stage II is absent at all test temperatues.

As the long-range order parameter η changes in single crystals and polycrystals the
stress–strain curves and the parameter of the stages are gradually transormed from one limit-
ing case (LRO) to the other limiting case (SRO), which is illustrated in Fig. 3.

Let us consider the effect of different factors on the hardening characteristics. In
polycrystals as the average grain size (<d>) increases, the beginning of each subsequent
stage shifts to larger deformations and, hence, the length of each stage increases. In the
alloy Ni_3Fe these situations are realized over a wide range of grain size without exception.
At the same time the stress corresponding to the beginning of the respective stages decreases
as <d> increases. In the disordered state of the alloy Ni_3Fe such an increase is observed
over the entire range of grain sizes studied while in the ordered state σ_{II} does not depend
on <d> and σ_{III} and σ_{IV} cease to change at a grain size greater than 150 μm.

The most important characteristic of the hardening stages is the hardening coefficient
$\Theta = d\sigma/d\varepsilon$. We found that in the ordered state of the alloy Ni_3Fe the coefficients Θ_{II}, Θ_{III},
and Θ_{IV} (for stages II, III, and IV, respectively) are virtually independent of the grain
size. In the disordered state only Θ_{IV} is independent of <d>. We should emphasize that the
fact that the hardening characteristic is independent of the grain size is a property of
stage IV. In the disordered state hardening in stage II decreases as the grain size grows,
especially at small grain sizes, and Θ_{III} is larger at smaller grain sizes. As a result of
this in stage IV the hardening coefficients for different grain sizes are equalized.

Let us briefly note the principal laws that govern how the parameters specifying the
stage nature of the process vary with the deformation temperature and the orientation of the
crystals. Any stage becomes shorter as orientation is shifted from the [001] corner to the
right part of the principal stereographic triangle. Such behavior is observed in both the
ordered and disordered states of Ni_3Fe. In the ordered alloy these parameters depend weakly
on the temperature. In the disordered alloy as the temperature rises, the beginning of stage
II shifts to smaller deformations, that of stage III shifts to larger deformations, while
that of stage IV does not move. Stage II becomes longer with rising temperature while stage
III becomes shorter. The stress at the beginning of stages II, III, and IV becomes sub-
stantially lower with decreasing number of octahedral systems with the same load in the fol-
lowing chain of orientations studied $[001] \rightarrow [119] \rightarrow [\bar{1}11] \rightarrow [011] \rightarrow [1.8.12]$. The quantities
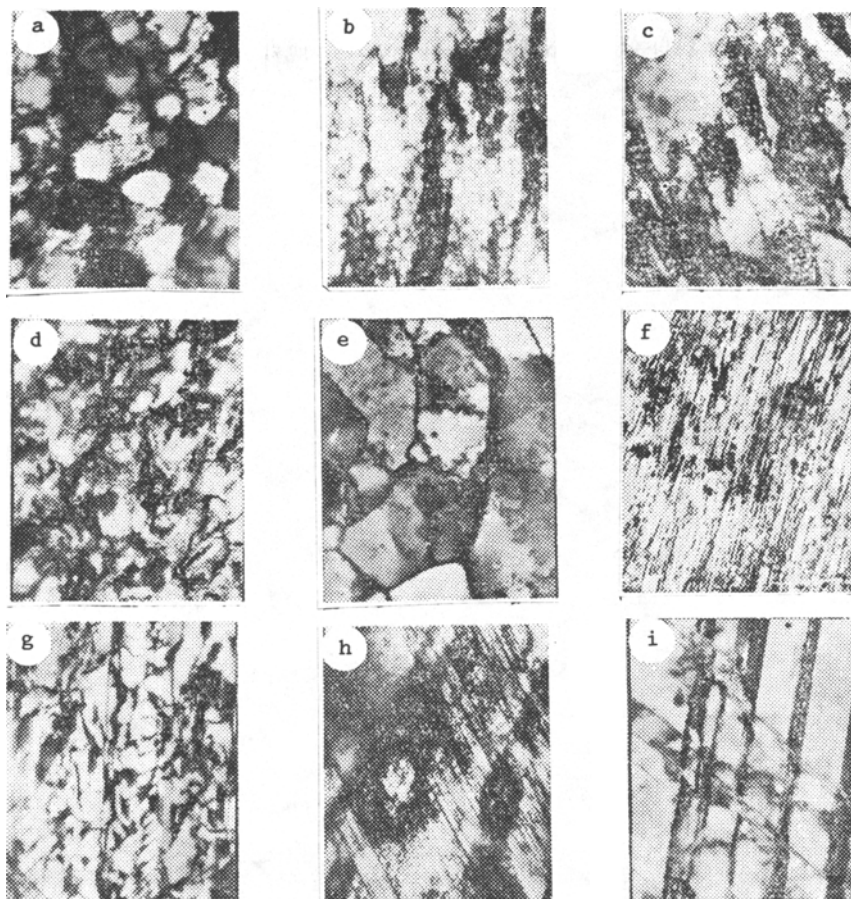either decrease or remain constant as the temperature of the test rises.

Fig. 5. Examples of types of misoriented substructures.

2. QUALITATIVE CHANGES IN THE DISLOCATION STRUCTURE — THE CAUSE
OF STAGES IN PLASTIC FLOW

Classification of Dislocation Substructures and the Sequence of Their Evolution. Electron-microscopic studies on different fcc alloys of solid solutions revealed that all the types of dislocation substructures (DSS) observed can be divided into two larger classes [16, 22, 23]: 1) the class of non-misoriented substructures and 2) the class of misoriented substructures. Discrete misorientations may occur in substructures of the first class but they are less than 0.5°. Among such non-misoriented dislocation substructures we distinguish (Fig. 4): a) randomly distributed dislocations (1); b) pileups (2); c) a uniform net structure (3); d) dislocation tangles (4); e) non-misoriented cells (5); and f) cellular-net substructure (7).

As misoriented substructures (the discrete misorientations at the subboundaries exceed 0.5°) we classify (Fig. 5): a) cellular substructure with misoriented (6), b) cellular-net dislocation structure with smooth misorientations (8); c) banded substructure (9); d) substructure with multidimensional discrete and smooth misorientations (10); and e) fragmented substructure (11). There is one more class of substructures, associated with twinning and martensitic transformations. The initial substructure in this class, a substructure with extended dislocations (12), can be classified as being misoriented (f). Incomplete twinning results in substructures (13) with multilayer stacking faults (g). They belong to the class of misoriented substructures. The twinning substructure (14) (one-, two-, or multi-dimensional) and the substructure with deformed martensite (15) (Fig. 5h and i, respectively) are misoriented substructures. The complete classification is given in Table 2. The numbers of the substructures are the same in the text and in Table 2.

In the form given above the classification of substructures is original. It was based on [24-30] and work done by us and our coworkers. Different types of dislocation substructure form, depending on the composition of the alloy, the energy of the stacking fault, the

TABLE 2. Classification of Substructures

Non-misoriented		Misoriented	
uniform	nonuniform	nonuniform	
dislocation		dislocation-disclination	dislocation-free
1. Random 2. Pileups 3. Net	4. Tangle Cellular (5, 6) 5. Nonmis-oriented 6. Misoriented Cellular-net (7; 8) 7. Nonmis-oriented 8. Misoriented	Subboundary 9. Banded (one- and two-dimensional) 10. Substructure with multidimensional continuous and discrete misorientations	11. Fragmented (subboundary)
		twinning, martensitic, etc	
12. Substructure with extended locations	13. Substructure with multiplayer stacking faults	14. Twinning (one- and multidimensional) 15. Substructure with deformed martensite	

states of atomic order, the degree of deformation, and the temperature. Analysis of the observed substructures showed that non-misoriented substructures arise under moderate deformations and misoriented substructures do under large deformations. The latter contain broken boundaries of degrees of perfection and, accordingly, are called dislocation—disclination substructures [31].

As the deformation develops the deformation substructures considered in the classification above arise not randomly but in a certain sequence, one after the other. The principal scheme of transformations for the case of dislocation and dislocation-disclination substructures is given in Fig. 6 [32]. Two main chains of transformations occur, one of which is characteristic of low or high alloys with a high stacking-fault energy and ordered alloys while the other is characteristic of concentrated alloys with a short-range order and a low stacking-fault energy. At high dislocation densities the two chains merge. The scale of the scalar dislocation density has a rather definite nature: despite the great diversity of the alloys the spread of the values along the scale is less then 1.5. The number does not change even if pure metals or other modes of deformation (e.g., fatigue) are included in the discussion. This indicates that the scalar dislocation density is an important parameter, which controls the evolution of the dislocation substructure.

Some changes in specific alloys are possible, depending on their properties and the deformation temperature. Hence, at elevated temperatures in pure metals or in alloys a cellular substructure may be followed immediately by a fragmented substructure, which in other cases may form after the banded structure. Since the average scalar dislocation density decreases when a fragmented structure is formed the position of this substructure in the scheme is arbitrary. A similar scheme can be drawn in the case of twinning a martensitic transformation.

Plastic Flow Stages and Corresponding Types of Dislocation Structures. The deformation hardening characteristics and the types of dislocation substructures can be related quantitatively. This can be done by using many transmission electron micrographs of thin foils to determine the volume fraction occupied by one type of dislocation structure or another. Quantitative measurements are thereby carried out at the structural level of the dislocation ensemble. These data along with the stress—strain curves and the hardening characteristics are shown in Fig. 7 for Ni_3Fe single crystals and polycrystals [14-17, 19, 32].
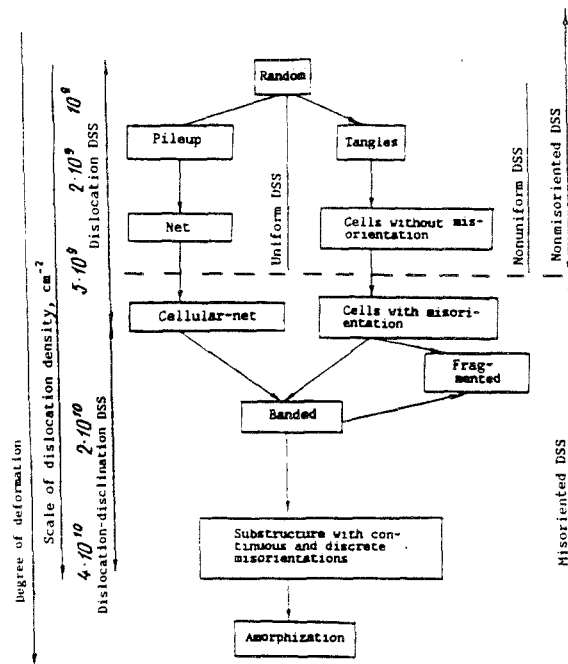
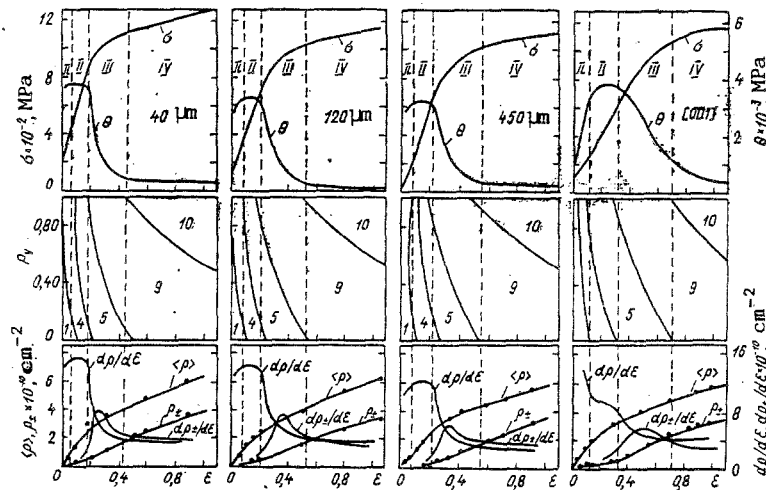Fig. 6. Scheme of transformations of sub-
structures.

Fig. 7. Stress—strain (σ vs ε) curves, Θ vs ε curves, diagrams
of P_V vs ε substructures and accumulation of scalar (ρ and $d\rho/d\varepsilon$)
and excess (ρ_+ and $d\rho_+/d\varepsilon$) dislocation densities with deformation
in polycrystals with different grain sizes (indicated on graphs)
and [001] single-crystals of Ni_3Fe alloy with long-range atomic
order.

As we see, two types of substructure, as a rule, exist at each stage of deformation in
a material. As the deformation develops, within the limits of the pertinent stage the volume
fraction of one of them decreases and that of the other increases. For example, in stage II
or the ordered alloy with the development of deformation the volume fraction of the tangle
substructure decreases and that of the cellular substructure increases. (In the disordered
alloy pileups are replaced by network of dislocations.) Completion of the stage coincides
with the disappearance of one type of substructure and the occupation of the entire volume
of the materials by the other type. The next, new type of substructure then appears and a
new stage begins. In stage III in the ordered alloy the volume fraction of the cellular sub-
structure diminishes and that of the banded structure grows. Stage IV in this material
begins when the banded substructure occupies the entire volume of the materials and begins
to transform into a substructure with discrete and smooth misorientations.
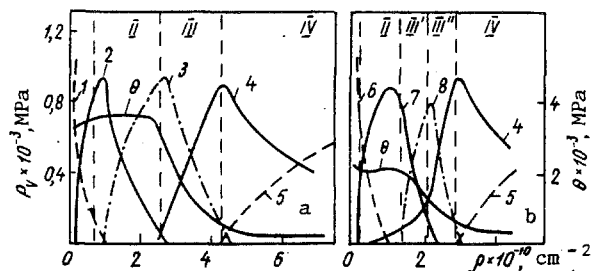
171

Fig. 8. Volume fraction (P_V) of substructures as a function
of the scalar dislocation density (ρ) in polycrystals of
Ni$_3$Fe alloy with a long-range order (a) and a close-range
order (b). The graphs for different grain sizes (40, 120,
and 450 µm) coincide. The Θ vs ε curves are also shown. The
dashed lines indicate the deformation stages [32].

Thus, the most general detail of the above picture of the interchangeability of the
stages in the deformation is that two types of dislocation substructure exist in each state,
i.e., that a "two-phase" defect subsystem exists at the level of the dislocation ensemble.

The diagrams of the structural states, drawn on the basis of studies of both Ni$_3$Fe
single crystals of different orientations [20] and polycrystals of alloy based on iron and
copper, are similar in nature [33, 34]. Naturally, other types of substructures are found
when there is a tendency toward twinning. All of the above laws of formation of stages re-
main valid.

The results reported here are evidence that the stages of plastic deformation appear
in accordance with the laws of evolution of the dislocation substructures. As a
result of this the level of the dislocation ensemble is the main structural level
that is responsible for the occurrence of the deformation in appearance, develop-
ment, and change of stages of the plastic deformation. Other structural levels
affect this process, but not immediately. Their effect stems from the factors that
determine the possible formation of one or other type of substructure. With increasing
grain size and transition to a single crystal the appearance of each subsequent substruc-
ture and the corresponding new stage shifts to higher degrees of deformation. Not infrequently
new substructures are nucleated in the boundary regions of grains. The hypothesis that a
change of substructures entails a change of stages is confirmed in studies by Trefilov et
al. [35, 36].

The volume fractions of the respective substructures as a function of the average scalar
dislocation density are given in the usual form in Fig. 8 [32]. In this representation we
clearly see that the corresponding type of substructure diminishes and grows at each stage as
well as that the end of each stage coincides with the disappearance of the preceding sub-
structure, the maximum volume of the existing substructure, and the formation of a new sub-
structure. Similar results were recently obtained on nickel single crystals [37]. Another
important feature of Fig. 8 is that the data for different grain sizes fit on one curve.
This indicates that the average scalar dislocation density is an important parameter which
controls the evolution of the dislocation substructure and the occurrence of plastic flow
in stages. In each state of order, regardless of the grain size, a new type of substructure
arises and so does a new stage of plastic deformation when a certain critical dislocation
density is reached.

Accumulation of Dislocations and the Quantitative Characteristics of the Dislocation
Structure. The quantitative characteristics of the dislocation structure and especially
their rate of change with the deformation turn out to be intimately bound up with state
nature of the plastic-flow curve. Information about the scalar density and rate of change
of the dislocations (along with the characteristics of the excess dislocation density) are
shown in Fig. 7. The measurements were made on Ni$_3$Fe single crystals and polycrystals in
the ordered and disordered states [14-17, 19, 32]. Obviously, the scalar dislocation den-
sity $\rho(\varepsilon)$ varies symbatically with the flow stress $\sigma(\varepsilon)$ and its rate of changed $d\rho/d\varepsilon$, with
the hardening coefficient Θ. The rate at which dislocations are accumulated reaches a max-
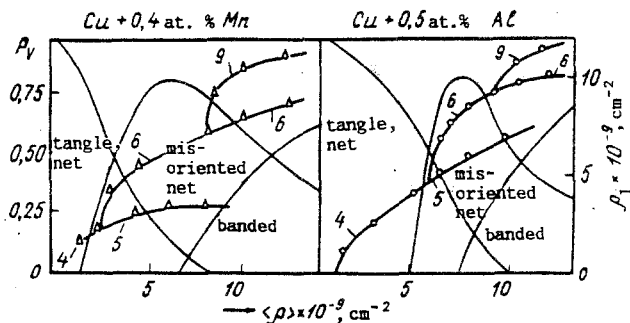imum in stage II, decreases abruptly in stage III, and reaches a constant (low) value in stage

Fig. 9. Volume fraction P_V of substructures (thin lines) and local dislocation density ρ_1 (thick lines) in different substructures as a function of the average scalar dislocation density in copper alloys. The numbers next to the ρ_1 vs $\langle\rho\rangle$ curves correspond to the notation for substructures in Table 2. The results were obtained with the collaboration of L. I. Trishkina.

IV. The decrease in this rate is due to the intensive development of annihilation of dis- locations during the formation of misoriented structures.

By virtue of the conditions under which the next chain of substructures is formed the dislocations are distributed nonuniformly in the volume of the material. The locally measured scalar dislocation density (ρ_1) for individual components of the substructure, i.e., in different types of coexistent dislocation substructures, is different. It is always higher in each subsequent substructure in comparison with its predecessor. An example for copper alloys is shown in Fig. 9.

The dislocation density measured near grain boundaries and inside grains differs. It is always high in boundary portions, i.e., where as a rule a new type of substructure begins to form in polycrystals. At the same time the contribution of this structural level is one cause of the smearing of the patterns of the stage nature of the process in polycrystals.

In the case of a cellular substructure variation of its parameters, such as the cell size and the width of the cell wall, also correlate with the stages of the deformation. The cell size decreases in the second stage and reaches saturation in the third stage, when this substructure begins to disappear [14, 16, 19]. In copper alloys the width of the cell walls increases in the second stage and reaches saturation in the third [34].

The parameters of the dislocation structure, which describe it in a scalar representation, thus vary in correlation with the stages of the deformation.

Excess Dislocation Density Lattice Curvature-Twist, and Elastic and Plastic Rotations at Different Structural Levels. In the stage of misoriented substructures the scalar description of the dislocation structure proves to be inadequate and it is necessary, at least, to introduce a new parameter, the excess dislocation density $\rho_\pm$. The local excess dislocation density

$$\rho_\pm = \rho_+ - \rho_- = \frac{1}{b}\frac{\partial\varphi}{\partial l} = \frac{\varkappa}{b} = \frac{1}{ab} \tag{1}$$

can be either a purely plastic bend determined from its gradient $\partial\varphi/\partial l$ [38]. In this case the excess dislocation density is directly related to the radius of curvature a and the average lattice curvature-twist $\varkappa$. The procedure for measuring these quantities has been expounded in detail in [14, 15, 29, 39].

The excess dislocation density $\rho_\pm$ and accumulation rate $d\rho_\pm/d\varepsilon$ for samples of the alloy Ni_3Fe are shown in Fig. 7 [14, 15, 19, 32]. This characteristic indicates the degree of polarization of the spatially distributed dislocation charge and is a local quantity. The formulas given above are determined by the modulus of this characteristic. The excess dislocation density begins to differ substantially from zero by the end of the stage II. Its accumulation rate reaches a maximum at the midpoint of stage III and drops to a constant by the beginning of stage IV. The appearance of excess dislocation density indicates the development of processes of annihilation of dislocation with opposite signs. The development of

cross slip abruptly activates these processes in stage III. The lowering of the accumulation rate of the scalar dislocation density is related precisely to the intensive annihilation of dislocations of opposite sign. The similarity of the accumulations of these scalar ($d\rho/d\varepsilon$) and excess ($d\rho_{\pm}/d\varepsilon$) dislocation densities by the beginning of stage IV indicates that almost all the dislocations appearing in this stage are annihilated and only an excess of dislocations of one sign persists in local volumes.

The accumulation of excess dislocation density thus also correlates with the stages of deformation hardening. On the basis of Eq. (1) such a conclusion can also be made in relation to the lattice curvature-twist ($\varkappa$).

When misoriented dislocation-disclination substructures are formed a variety of subboundaries is formed after the appearance of excess dislocation distribution in the volume. The variation of the quantitative characteristics of misoriented substructures also correlates with the stages of the deformation [14, 19, 39, 40]. The distances between condensations and their width in the cellular-net substructure decrease in stage III and remain virtually constant in stage IV. The density of the subboundaries of the banded substructure grows more rapidly in stage III than in stage IV. Disclination loops and both azimuthal and radial misorientations exhibit the same behavior.

Let us consider the role of structural levels in the manifestation of lattice turns. In different stages of deformation, when the misorientation gradients are low, misorientations appear at the level of grains in the polycrystalline material, within which continuous misorientations can reach several degrees. Upon transition to stage III continuous and discrete misorientations are realized at the structural level of the dislocation ensemble, portions of a grain, cell, band, or disclination loop, as well as individual subboundaries. The misorientation gradients determined from the bend contours coincide with those found from the bend of the bands in the banded substructure. On the whole, with the development of deformation the pattern of misorientations becomes more involved and more inhomogeneous, their scale becomes smaller, and at the same time a tendency toward the development of a scale hierarchy of misorientations manifests itself.

The transition from stage III to stage IV is linked to the abrupt development of inhomogeneties in the pattern of misorientations. The banded substructure changes from one-dimensional to multi-dimensional and the bands become highly curved and split up. The subboundaries limiting the bands are transformed from pure tilt or twist boundaries into mixed boundaries and a gradient of discrete misorientation appears in them. The gradient of the lattice bend-twist, which was parallel to the subboundaries in stage III, abruptly changes direction and becomes a local and inhomogeneous quantity. In such complex substructures the excess dislocation density becomes an insufficiently informative quantity and the bend-twist tensor or the dislocation-density tensor must be used to characterize the continuous misorientation [39, 40]. According to our measurements, in stage III, as a rule, one or two components of the bend-twist (dislocation density) tensor are locally nonzero and their amplitudes increase with the deformation. In stage IV the growth of the amplitude slows down abruptly and then the number of nonzero tensor components begins to grow, i.e., the nature of the lattice bend-twist becomes more involved because of the accumulation of excess density of dislocations with different Burgers vectors.

3. STRUCTURAL LEVELS AND STAGES OF PLASTIC DEFORMATION

Analysis of the Role of Different Structural Levels in the Formation of the Defect Structure and Localization of Slip. In the preceding sections we have already basically considered the role of microscopic and mesoscopic structural levels in the processes of slip and defect formation. The transition was completed from the properties of individual defects to properties of the dislocation ensemble as the most important transition for the development of a uniform plastic deformation of the structural level. The large-scale levels in turn affect these processes. This is due primarily to the laws of deformation of grains and groups of grains.

In stage II the effect of the structural level of the grain and its neighbors (parts of a grain or groups of grains) is scanned especially well [41, 49]. The main contribution to the deformation and accumulation of dislocations is made by primary systems (one or two), loaded with the highest external stress. The shear intensity in them and the relative shear are proportional to Schmid's factor [41-43]. Accommodation systems act near grain boundaries. Their activation is due to contact stresses caused by the mismatch of the deformation of neigh-

boring grains and the continuity of the material is preserved by the action of these systems. At the places where they act, i.e., in boundary regions, the dislocation density is higher than in the body of the grain.

As the deformation develops, especially in the transition to stage III, secondary slip arises along less loaded systems in the body of the grain. This development during stage III and the evolution of the intragrain structure weaken the effect of the structural level of the grain while in stage IV, they cause it to switch off completely. This is illustrated well by the pattern of accumulation of the scalar and excess dislocation density (see Fig. 7). In the transitional stage and in stage II dislocations are accumulated more rapidly in samples with a small grain size. In stage III the effect of the average grain size at first reverses its nature and then weakens while in stage IV it is absent altogether. Such behavior is also characteristic of the accumulation of excess dislocation density.

The cells of the cellular substructure grow with increasing average grain size in stage II but this dependence attenuates in stage III. For the cellular-net substructure in stage III the distance between condensations is greater when the grain size is large but in stage IV the effect of the grain size virtually vanishes. Only for the banded substructure does the subboundary density increase as the grains become smaller in both stage III and stage IV but in this case the effect of the given structural level weakens.

The effect of other structural levels also manifests itself in the laws of deformation of a polycrystalline aggregate. First, there is the role of the individual grain size from the grain size distribution function [43, 50]. As a result of the combined effect of a number of factors, as the deformation increases the large grains of a given sample make a larger contribution to the elongation than do small grains. Second, the more grains enter into a group, the more slowly the deformation of this group becomes more nonuniform with increasing elongation. A correlation is observed in the deformation of small groups of grains (3-6 grains). Third, some structural levels are found to affect other levels. The more localized the deformation is at the level of the shear zone, the more nonuniform the deformation is at such large-scale structural levels as a grain, group of grains, macroscopic parts of the sample, and the samples as a whole [43].

Critical Dislocation Density, Interdislocation Interaction, and Self-Organization of Dislocation Structures. Each type of substructure exists in a certain range of dislocation densities and this range is not only constant for one material (Fig. 6), but changes little in the transition from one material to another and when the mode of deformation changes. Each type of substructure is formed not only and not so much as under the effect of external stresses (the latter causes development of slip and generation of dislocations in the volume of the material) and as a result of dislocation redistribution under the effect of the forces of interdislocation interaction. As the scalar density of dislocations increases the distance between them decreases more and more and the forces of interdislocation interaction begin to form substructures of the respective class, while the role of collective phenomena grows accordingly [30, 44]. They cause the corresponding substructure to form.

Each type of dislocation substructure, as is seen from Fig. 6, appear at some value of the scalar dislocation density ρ, which may be called the critical value ρ_{cr}. The concept of the existence of a critical dislocation density for the formation of substructures was introduced theoretically in [30, 45-47] and as a result of experimental studies in [48].

The driving force of the process of rearrangement of dislocation substructures is a tendency toward a relative minimum of the total energy of the dislocation subsystem [32, 49, 50]. It consists of the energy of individual dislocations and the energy of their interaction. When one substructure is transformed into another both contributions change so that at a given dislocation density the energy of the new reconstituted substructure is below that of the predecessor [32].

The main contribution to the energy of the substructure is made by the elastic energy ΔU of the dislocations:

$$\Delta U = \frac{\rho G b^2}{4\pi} \ln \frac{L}{r_0} . \tag{2}$$

Here r_0 is the radius of the dislocation core and L is the screening radius of the elastic field of the dislocations. The latter is the most important quantity in the problem in the
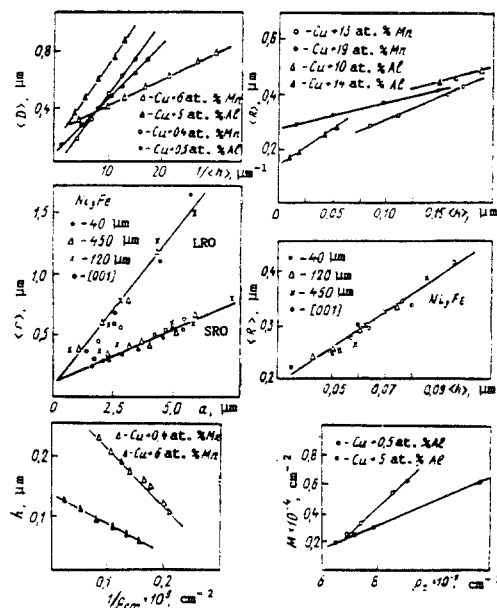
Fig. 10. Interrelationship between
the parameter of different substruc-
tures: R is the distance between
condensations of dislocations in a
cellular-net substructure; D is the
cell size in a cellular DSS; h is
the width of condensations in a cel-
lular-net structure or the wall width
in a cellular structure; r is the
distance between subboundaries in a
banded substructure; a is the radius
of lattice curvature; M is the dens-
ity of broken subboundaries; $\rho\pm$ is
the excess dislocation density; ρ_w
is the dislocation density in the
cells walls [32, 40].

formation of a sequence of substructure transformations. In the diagram in Fig. 6 it de-
creases in substructures in order of increasing scalar dislocation density, at least for those
dislocations which participate in the formation of the characteristic features of each new sub-
structure: chaos, tangles, cells walls, and subboundaries of the banded substructure. The
quantity L is of the order of the grain size for a chaotic substructure, of the order of the
cell-wall width or width of condensations for cellular or cellular-net substructures, and
of the order of the interdislocation distance in the subboundaries for a banded substructure.
The transition to misoriented substructures gives rise to dislocation charges with a sub-
sequent reduction of the result of the alternation of the sign of the charge in their spa-
tial arrangement and a reduction of the substructure parameters.

This nature of the processes in the formation of the dislocation substructures attests
to self-organization. The existence of a process of self-organization is proved by the
existence of functional relations between the substructure parameters. The simplest form
of dependence is a linear one. Thus in a cellular substructure the cell size is related to
the reciprocal of the cell width, in a cellular-net substructure the distance between con-
densations is related to their width, and in a banded substructure the distance between sub-
bounderies is related to the radius of the lattice curvature-twist (Fig. 10) [32, 40].

Phase Transformations in the Defect Subsystem and the Nature of the Stages of Plastic
Deformation. The laws of the evolution of the defect substructure allow it to be considered
in a number of cases as an almost independent subsystem of the deformed material. In this
case besides the temperature and external stress, the average scalar dislocation density
is an important parameter that controls the behavior of this subsystem. When a new substruc-
ture is formed there appear new parameters which describe it and which were either not present
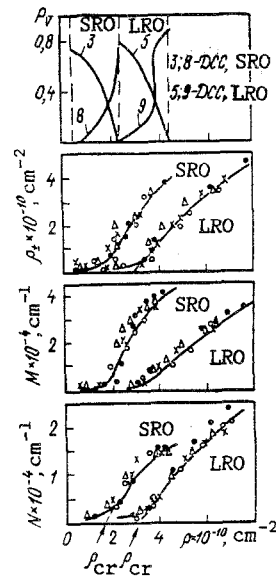
Fig. 11. Phase transition in the dis-
location structure of polycrystals with
a grain size of 40 (•), 120 (Δ), and
450 (×) μm and [001] single crystals (o)
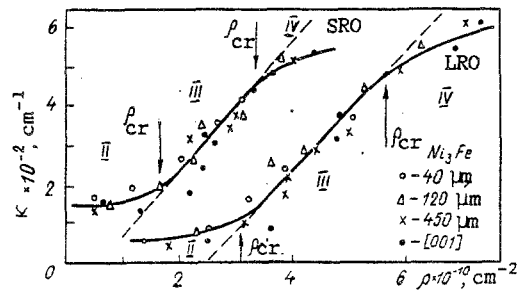of the alloy Ni$_3$Fe [32].

Fig. 12. Variation of the curvature
κ of the defect lattice with increas-
ing scalar dislocation density [40].

in the previous substructures or were not characteristic of them. Such parameters can be used as parameters of the transition from one substructure to another.

From this standpoint let us consider the transformations between non-misoriented and misoriented substructures. As is clear from the discussion above, this transformation has the nature of a kinetic phase transformation [23]. This is particularly distinct in analysis of data on the alloy Ni$_3$Fe. The volume fractions of the old, decaying substructure and the new, developing substructure (which are non-misoriented and misoriented, respectively, depending on the scalar dislocation density) are given in Fig. 11. In these coordinates the volume fraction and all the subsequent characteristics lie on one curve for both single crystals and polycrystals with different grain sizes. This is why the scalar dislocation density <ρ> can be adopted as a parameter of the system. The two-phase nature of the transformation is visible clearly in the substructure itself. An interface of finite thickness (∿0.3 μm) exists between the portions of the banded and cellular substructures.

Any quantities characterizing the misorientation, such as the excess dislocation density ρ$_+$, the lattice curvature-twist, the subboundary density M, the misorientation at those subboundaries, the density of extinction contours N, etc., can be parameters of the transformation in the case under consideration. Some of them (ρ$_+$, M, N) are shown in Fig. 11. The meaning of the critical dislocation density ρ$_{cr}$ is clear, viz., the new parameter of the defect subsystem increases abruptly at this value. At the same time a new stage of plastic deformation begins. The observation of a kinetic phase transition is the clearest proof of processes of substructure self-organization. The transitions between other types of

substructures can be represented as phase transitions in the defect subsytem. Let us consider the transition between a banded substructure and a structure with discrete and continuous misorientations. A kink observed on the curves in Fig. 11 at large values of the scalar dislocation density correspond to it. It is particularly visible in $\kappa(\rho)$ coordinates in Fig. 12 [40], from which it follows that the lattice curvature can be a parameter of the transformations that lead to both the formation and disappearance of the banded substructure. The essence of the last phase transition lies in the abrupt slowing down of the growth of amplitude of the lattice curvature-twist, which is changed by an increase in the number of nonzero components of the lattice curvature-twist tensor.

CONCLUSION

In summary, the transition from one stage of plastic deformation to another is due to the phase transformations in the subsystem of deformation defects. These transformations are controlled by an internal parameter of the system, viz., the scalar dislocation density, whose value is determined by both the external force and processes retarding the shear and annihilation. The main structural level controlling this process is the level of the dislocation subsystem.

LITERATURE CITED

1. A. Seeger, Dislocation and Mechanical Properties of Crystal [Russian translation], IL, Moscow (1956).
2. L. M. Clareborough and M. F. Hargreaves, Advances in Metal Physics [Russian translation], Metallurgizdat, Moscow (1936).
3. R. Berner and G. Kronmüller, Plastic Deformation of Single Crystals [Russian translation], Mir, Moscow (1969).
4. V. R. Regel', Itogi Nauki, Fiz.-Mat. Nauki, Net. Vpr. Fiz. Plast. Metallov, Izd. Akad. Nauk SSSR, No. 3, 12 (1960).
5. L. E. Popov, N. A. Koneva, and I. V. Tereshko, Strain Hardening of Ordered Alloys [in Russian], Metallurgiya, Moscow (1979).
6. L. E. Popov and N. A. Koneva, Izv. Vyssh. Uchebn. Zaved., Fiz., No. 8, 132 (1976).
7. V. E. Panin, Yu. V. Grinyaev, T. F. Elsukova, and A. G. Ivanchin, Izv. Vyssh. Uchebn. Zaved., Fiz., No. 6, 5 (1982).
8. V. E. Panin, V. A. Likhachev, Yu. V. Grinyaev, Structural Levels of Deformation of Solids [in Russian], Nauka, Novosibirsk (1985).
9. N. A. Koneva, L. A. Teplyakova, V. A. Starenchenko, and É. V. Kozlov, Izv. Vyssh. Uchebn. Zaved., Fiz., No. 10, 24 (1977).
10. N. A. Koneva, L. A. Teplyakova, V. A. Starenchenko, and É. V. Kozlov, Fiz. Met. Metalloved., 48, No. 3, 613 (1979).
11. N. A. Koneva, L. A. Teplyakova, V. A. Starenchenko, et al., Fiz. Met. Metalloved., 49, No. 3, 620 (198).
12. S. P. Zhukovskiĭ, N. A. Koneva, V. S. Kobytev, et al., Izv. Vyssh. Uchebn. Zaved., Fiz., No. 2, 35 (1981).
13. N. A. Koneva, L. A. Teplyakova, and É. V. Kozlov, Structure and Plastic Behavior of Alloys [in Russian], A. F. Ioffe Physicotechnical Institute, Leningrad (1984).
14. N. A. Koneva, D. V. Lychagin, S. P. Zhukovskiĭ, and É. V. Kozlov, Fiz. Met. Metalloved., 60, No. 1, 171 (1985).
15. V. A. Koneva, D. V. Lychagin, L. J. Trishkina, and E. V. Kozlov, Strength of Metals and Alloys: Proceedings of ICSMA-7, Montral, Canada, August 12-16, 1985, Pergamon Press, Oxford (1985), Vol. 1, pp. 21-23.
16. N. A. Koneva, D. V. Lychagin, O. B. Perevalova, and S. P. Zhukovskii, in: Plastic Deformation of Alloys [in Russian], Tomsk State University, Tomsk (1986).
17. N. A. Koneva, D. V. Lychagin, O. B. Perevalova, and S. P. Zhukovskii, in: Plastic Deformation of Alloys [in Russian], Tomsk State University, Tomsk (1986).
18. L. A. Teplyakova, N. A. Koneva, D. V. Lychagin, et al., Izv. Vyssh. Uchebn. Zaved., Fiz., No. 2, 18 (1988).

19. L. A. Teplyakova, N. A. Koneva, D. V. Lychagin, et al., Izv. Vyssh. Uchebn. Zaved., Fiz., No. 2, 18 (1988).
20. A. V. Paul' and N. A. Koneva, in: Substructure and Mechanical Properties of Metals and Alloys [in Russian], Tomsk State University, Tomsk (1988).
21. T. S. Kunitsyna, L. A. Teplyakova, and N. A. Koneva, in: Substructure and Mechanical Properties of Metals and Alloys [in Russian], Tomsk State University, Tomsk (1988).
22. N. A. Koneva and É. V. Kozlov, Izv. Vyssh. Uchebn. Zaved., Fiz., No. 8, 3 (1982).
23. N. A. Koneva, D. V. Lychagin, L. A. Teplyakova, and É. V. Kozlov, in: Theoretical and Experimental Study of Disclinations [in Russian], A. F. Ioffe Physicotechnical Institute, Leningrad (1986).
24. A. Howie, Direct Observation of Imperfections in Crystals [Russian translation], Metallurgiya, Moscow (1964).
25. P. Hirsch, New Electron-Microscopic Studies [Russian translation], Metallurgiya, Moscow (1961).
26. J. W. Steeds, Proc. R. Soc. London, 292, 343 (1966).
27. A. N. Vergazov, V. A. Likhachev, and V. V. Rybin, Fiz. Met. Metalloved., 42, No. 1, 146 (1976).
28. V. I. Trefilov, Yu. V. Mil'man, and S. A. Firstov, Physical Foundations of the Strength of Refractory Metals [in Russian], Naukova Dumka, Kiev (1975).
29. V. S. Ivanova, Fracture of Metals [in Russian], Metallurgiya, Moscow (1979).
30. V. V. Rybin, Large Plastic Deformations and Fracture of Metals [in Russian], Metallurgiya, Moscow (1986).
31. V. I. Vladimirov (ed.), Disclinations. Experimental Studies and Theoretical Description, A. F. Ioffe Physicotechincal Institute, Leningrad (1984); (1984); (1986).
32. N. A. Koneva, D. V. Lychagin, L. I. Trishkina, and É. V. Kozlov, in: Physical Aspects of Prediction of Fracture and Formation of Heterogeneous Materials [in Russian], A. F. Ioffe Physicotechnical Institute, Leningrad (1987).
33. L. I. Trishkina and É. V. Kozlov, in: Substructure and Mechanical Properties of Metals and Alloys [in Russian], Tomsk (1988).
34. N. A. Koneva, L. I. Trishkina, G. V. Daneliya, and É. V. Kozlov, Fiz. Met. Metalloved., 66, No. 4, 808 (1988).
35. V. I. Trefilov, I. D. Gornaya, V. F. Moiseenko, et al., Dokl. Akad. Nauk UkrSSR, Ser. A, No. 5, 83 (1980).
36. V. I. Trefilov, V. F. Moiseev, and E. P. Pechkovskii, Strain Hardening and Fracture of Polycrystalline Metals [in Russian], Naukova Dumka, Kiev (1987).
37. V. A. Starenchenko, M. S. Tsarapkin, and V. S. Kobytev, in: Substructure and Mechanical Properties of Metals and Alloys [in Russian], Tomsk Polytechnical Institute, Tomsk (1988).
38. A. N. Orlov, Introduction to the Theory of Crystal Defects [in Russian], Vysshaya Shkola, Moscow (1983).
39. É. V. Kozlov, D. V. Lychagin, N. A. Popova, et al., in: Physics of the Strength of Heterogeneous Materials [in Russian], A. F. Ioffe Physicotechnical Institute, Lenigrad (1988).
40. N. A. Koneva, D. V. Lychagin, L. A. Tephyakov, et al., in: Disclination and Rotational Deformation of Solids [in Russian], A. F. Ioffe Polytechnical Institute, Leningrad (1988).
41. N. A. Koneva, S. P. Zhukovskii, I. A. Lapsker, and É. V. Kozlov, in: Solid-State Physics and Electronics [in Russian], Udmurtiya State Univeristy, Izhevsk (1982).
42. Yu. P. Sharkeev, I. A. Lapsker, N. A. Koneva, and É. V. Kozlov, Fiz. Met. Metalloved., 60, No. 4, 816 (1985).
43. N. A. Koneva, S. P. Zhukovskii, I. A. Lapsker, et al., in: Disclinations and Rotational Deformations of Solids [in Russian], A. F. Ioffe Physicotechnical Institute, Leningrad (1989).
44. V. I. Vladimirov and A. E. Romanov, Disclinations in Crystals [in Russian], Nauka, Leningrad (1986).
45. A. N. Orlov, Fiz. Met. Metalloved., 20, No. 1, 12 (1965).
46. D. L. Holt, J. Appl. Phys., 41, No. 8, 3197 (1970).
47. V. I. Vladimirov and A. A. Kusov, Fiz. Met. Metalloved., 39, No. 6, 1150 (1975).
48. V. S. Ivanova and V. F. Terent'ev, Nature of Metal Fatigue [in Russian], Metallurgiya, Moscow (1975).
49. "Low-energy dislocation structures," Mater. Sci. Eng., 81, 574 (1986).
50. D. Kuhlmann-Wilsdorf, Phys. Status Solidi A, 104, 121 (1987).